HHS Public Access

Author manuscript

Int J Radiat Oncol Biol Phys. Author manuscript; available in PMC 2016 November 15.

Published in final edited form as:

Int J Radiat Oncol Biol Phys. 2015 November 15; 93(4): 892–900. doi:10.1016/j.ijrobp.2015.07.2283.

A novel manganese-porphyrin superoxide dismutase-mimetic widens the therapeutic margin in a pre-clinical head and neck cancer model

Kathleen A. Ashcraft[1], **Mary-Keara Boss**[2], **Artak Tovmasyan**[1], **Kingshuk Roy Choudhury**[3], **Andrew N. Fontanella**[4], **Kenneth H. Young**[1], **Gregory M. Palmer**[1], **Samuel R. Birer**[1], **Chelsea D. Landon**[1], **Won Park**[1], **Shiva K. Das**[5], **Tin Weitner**[1], **Huaxin Sheng**[7], **David S. Warner**[7], **David M. Brizel**[1,8], **Ivan Spasojevic**[6], **Ines Batinic-Haberle**[1], and **Mark W. Dewhirst**[1,3]

[1]Department of Radiation Oncology, Duke University Medical Center, Durham, NC 27710

[2]North Carolina State College of Veterinary Medicine, Department of Molecular Biomedical Sciences, Raleigh, NC 27607

[3]Department of Biostatistics and Bioinformatics, Duke University, Durham, NC 27710

[4]Department of Biomedical Engineering, Duke University, NC 27710

[5]Department of Radiation Oncology, Physics and Computing Division, University of North Carolina School of Medicine, Chapel Hill, NC 27599

[6]Department of Medicine, Duke University Medical Center, Durham, NC 27710

[7]Department of Anesthesiology, Duke University Medical Center, Durham, NC 27710

[8]Department of Surgery, Duke University Medical Center, Durham, NC 27710

Abstract

Purpose—Normal tissue injury is dose limiting for radiotherapy (RT) in nearly every application. This provides strong rationale for developing new classes of novel radioprotectors. The caveat is that radioprotective drugs must be selective for normal tissue and not tumor. Here we tested the effects of a novel Mn porphyrin oxidative stress modifier, MnBuOE for its radioprotective and radiosensitizing properties in normal tissue vs. tumor, respectively.

Methods—Murine oral mucosa and salivary glands were treated with a range of radiation doses, ±MnBuOE to establish the dose effect curves for mucositis and xerostomia. Radiation injury was quantified by intravital NIR imaging of cathepsin activity, assessment of salivation and histological analysis. To evaluate effects of MnBuOE on the tumor radiation response, we

Corresponding Author: Mark W. Dewhirst, Department of Radiation Oncology, Duke University Medical Center, Box 3455, Medical Sciences, Research Building 1, Room 201, Durham, NC 27710, Phone: 919-684-4180, Fax: 919-684-8718, mark.dewhirst@duke.edu.

Conflict of Interest. No other authors have conflicts of interest related to this report.

administered the drug as an adjuvant to fractionated radiation of FaDu xenografts. Again, a range of RT doses were administered to establish the radiation dose effect curve. The TCD_{50} values ±MnBuOE and dose modifying factor were determined.

Results—MnBuOE protected normal tissue by reducing RT-mediated mucositis, xerostomia and fibrosis. The dose modifying factor for protection against xerostomia was 0.77. In contrast, MnBuOE increased tumor local control rates, compared to controls. The dose modifying factor, based on the ratio of TCD_{50} values, was 1.3. Immunohistochemistry showed that MnBuOE-treated tumors exhibited a significant influx of M1 tumor-associated macrophages, which provides mechanistic insight into its radiosensitizing effects in tumors.

Conclusions—MnBuOE widens the therapeutic margin by decreasing the dose of radiation required to control tumor, while increasing normal tissue resistance to RT-mediated injury. This is the first study to quantitatively demonstrate the magnitude of a single drug's ability to radioprotect normal tissue while radiosensitizing tumor.

Introduction

There are 50,000 cases of squamous cell head and neck cancer diagnosed in the United States annually. Two-thirds of these patients will receive RT with curative intent. However, RT often results in permanent xerostomia (loss of saliva production). Xerostomia impairs speaking and/or swallowing, increases the risk of dental caries, osteonecrosis of the mandible and malnutrition, and decreases patients' quality of life[1]. Further, significant oral and pharyngeal mucositis develops during RT of HNSCC. Mucositis adversely affects treatment delivery and patient nutrition and significantly increases the overall cost of care[2]. There are no FDA-approved agents for the management of mucositis and the only FDA-approved therapy for inhibiting xerostomia, amifostine, is unsuitable because of side effects and incomplete protection[3–5]. A strong and unmet medical need exists for safer and more effective radioprotecting agents.

Reactive oxygen (ROS) and reactive nitrogen species (RNS) formed after RT contribute to salivary gland cell death. NO and $O_2^{\bullet-}$ accumulate in the submandibular gland post-RT, and react to form toxic peroxynitrite ($ONOO^-$). This provides rationale to consider superoxide dismutase (SOD) as a therapy[6].

Our group has developed a potent manganese porphyrin-based superoxide dismutase (SOD) mimic and regulator of cellular redox-based signaling pathways, MnBuOE[7]. MnBuOE accumulates in mitochondria, a site of oxidative stress after RT[8]. Analogues of MnBuOE reduced injury following radiation induce erectile dysfunction[9], ocular hypertension[10], renal ischemia[11], pulmonary radiation injury[12–14], and spinal cord contusion[15]. In this paper, we compare the effects of MnBuOE on radiotherapy response of tumor using the FaDu HNSCC model vs. relevant normal tissues of the head and neck.

We show that MnBuOE widens the therapeutic margin for RT in this model of head and neck cancer by shifting the radiation response curves in opposite directions for tumor and normal tissue.

Methods

Salivary gland and oral mucosa irradiation

C57Bl/6 mice were anesthetized with 1.5% isoflurane gas mixed with oxygen and placed in an X-RAD 225Cx (Precision X-ray Inc., North Branford, CT) small animal micro-CT irradiator[16]. A collimating cone that produced a 15 mm × 40 mm radiation field was used to target the radiation beam to the salivary gland and oral cavity (Figure 1). The RT field included all major and minor salivary glands (located primarily in the neck region of mice[17]), and the oral mucosa, including glands of the cheeks, lips and tongue. The target tissues were localized within the radiation field with a source-to-subject distance of 30.76cm, using fluoroscopy at 40kVp and 2.5mA with a 2mm Al filter. The target area was irradiated using opposed lateral beams at a dose rate of 300cGy/minute at target depth with 225kVp and 13mA and a 0.3mm Cu filter. Control mice were anesthetized but not irradiated.

Fluorescence molecular tomography

Mice were injected i.v. with 100 μL ProSense 750EX (Perkin Elmer, Boston, MA). This probe fluoresces after cleavage by cathepsins and plasmin. Cathepsins have been implicated in mucositis because inhibitors alleviate chemotherapy-induced mucositis[18]. Twenty-four hours after injection, mice were anesthetized via isoflurane and imaged using the Visen FMT 2500LX (Perkin Elmer). The ProSense 750EX signal was determined using TrueQuant software (Perkin Elmer Life and Analytical Sciences, Downers Grove, IL).

Saliva collection

Mice were intraperitoneally injected with 3 μg carbomylcholine chloride (Sigma, St. Louis, MO) dissolved in sterile PBS. Salivation began two minutes after injection. Saliva was collected via pipet for four minutes. The volume was measured gravimetrically, assuming a density of 1 g/mL.

Tumor transplant and growth delay

1×10^6 FaDu cells were injected subcutaneously into the right flank of nude mice in a volume of 100 μL. MnBuOE started one week post-transplant and continued for 40 days. When tumor volumes reached 200–300mm^3, mice were randomized into RT dose groups (divided equally over 5 consecutive days). Tumors were measured daily with calipers, and volumes were calculated using the formula $V=(A^2xBx\pi)/6$, where A is the shortest diameter and B is the longest diameter. Mice were sacrificed when their tumor reached 1500mm^3.

Statistics

Time to endpoints for tumor growth (reaching 1500 mm^3) were analyzed using multivariate Cox regression[19], with a linear term for dose with an interaction with treatment (Saline or MnBuOE), with baseline being Saline at 0 Gy. The dose response of tumor control probabilities was modelled as a two parameter logistic[20] fitted by non-linear least squares. Animal-wise average salivation levels between weeks 2–4 were analyzed using a model with a quadratic effect of dose and an additive effect for treatment (MnBuOE), with baseline

being Saline at 0 Gy. All other group-wise comparisons were conducted using ANOVA. Pair-wise analyses of Masson's staining were done with a Student's t-test. All statistical analyses were carried out in the R computing platform (www.r-project.org) or GraphPad Prism 6 (GraphPad, LaJolla, CA).

Results

Pharmacokinetics and tissue levels of MnBuOE

The chemical structure of MnBuOE is shown in (Supplemental Figure 1)[7]. Pharmacokinetic studies were conducted on mice that received MnBuOE at various doses, injected subcutaneously, bi-daily (b.i.d). MnBuOE was rapidly cleared from circulation and plasma levels did not accumulate at doses less than 4.5 mg/kg b.i.d. (Supplemental Figure 2a). The accumulation at 9 mg/kg b.i.d. on day 28 may be explained by saturation in the liver and kidneys, which were previously shown to retain drug following clearance from the circulation. MnBuOE was detectable in the salivary gland, and levels were dose dependent and reached a steady state within the first week for doses of 4.5 b.i.d. and below (Supplemental Figure 2b). Detailed pharmacokinetic and biodistribution results of MnBuOE will be reported elsewhere (Tovmasyan et al., in preparation).

After 28 days of MnBuOE, there was no difference in body weight among groups (p=0.34) (Supplemental Table 1) and no impact on salivation (p=0.58) (Supplemental Table 2). Analogues with similar pharmacodynamic properties are therapeutically active at concentrations measured in the salivary gland, following a b.i.d. dose of 1.5mg/kg[13]. Thus, this dosing regimen was used for all studies.

Radioprotection of normal tissue

To determine whether MnBuOE protected normal tissue to RT, C57Bl/6 mice received a single fraction of varying doses of RT to the oral cavity and ventral neck region only (Figure 1). MnBuOE was administered using the same dose and schedule as the tumor control study, beginning one week prior to RT and continuing throughout the experiment.

Mucositis was assessed ten days post-radiation. As expected, mice that received 0Gy of radiation showed only background ProSense™ signal. Irradiation with 9Gy resulted in very low levels of inflammation. Control mice irradiated with doses of 11, 13, or 15Gy showed a dose dependent increase in inflammation (Figure 2a). Irradiated mice that received MnBuOE also showed evidence of inflammation, but it was less severe than that observed in the saline-treated mice. When the ProSense™ signal was quantified, MnBuOE significantly reduced mucositis (p=0.009) across RT groups (Figure 2b).

To assess xerostomia, the average saliva volume collected per mouse over weeks 2–4 post-RT is shown in Figure 3. We chose to collapse the data across weeks because each mouse's salivation nadir occurred at different times. There was no significant difference between groups for the 0 Gy controls. Saliva production decreased at all RT doses in the saline controls compared to both the 0 Gy controls and the MnBuOE treated mice at the same RT dose. When MnBuOE was administered, saliva production remained stable in the 9 and 11 Gy groups. Saliva production in the MnBuOE group was on average 26.2±6.8 μl/Gy higher

(p=0.0002) in the MnBuOE group relative to saline. Figure 3 The dose modifying factor for xerostomia was 0.77.

Masson's trichrome staining was used to assess salivary gland fibrosis at six weeks post-RT with 0 or 15Gy to determine if salivary function correlated with histologic changes. To quantify the bright blue areas representing fibrotic tissue, the percentage of blue pixels that had a green:red ratio of >0.1 was quantified. Figure 4 shows representative images from three mice per group, alongside the corresponding processed images which highlight the blue pixels. Radiation significantly increased fibrosis staining in the saline-treated control mice, compared to 0Gy/saline controls (p=0.0092). However, fibrosis was not increased in 15Gy/MnBuOE compared to the 0Gy/MnBuOE treated mice (p=0.69). Thus, preserved salivary function correlated with reduced fibrosis in the salivary glands.

Tumor radiosensitization by MnBuOE

FaDu xenografts were transplanted into the flanks of nude mice. Mice were treated with 5 fractions of 5, 6, 7.5, 9 or 10Gy. Multivariate Cox regression analysis of the time to tumor volume endpoint (1500 mm^3) revealed no significant effect of MnBuOE in affecting tumor growth at 0Gy (p-value=0.91). (Figure 5a). Increasing radiation dose had a highly significant effect on the hazard of local failure (p-value < 0.0001). However, addition of MnBuOE lowered the hazard of failure at higher doses (p=0.02). This was evident by several analyses. First, there was an increase in time to 1500mm^3 in mice treated with 5x5Gy and 5x6Gy +MnBuOE compared to mice receiving 5x5Gy and 5x6Gy+saline. For the 5x7.5Gy and 5x9Gy treatment groups, only saline control mice reached the 1500mm^3 endpoint (3 and 4 mice, respectively). No mice that were treated with 5x7.5Gy or 5x9Gy in the presence of MnBuOE reached the 1500mm^3 endpoint. No mice in either the saline or MnBuOE group reached endpoint following 5x10Gy.

A second difference between treatments related to tumor regression and recurrence (Supplemental Figure 3a). For 5x7.5Gy, tumors regressed in 6/10 saline and 8/9 MnBuOE treated mice. Of the regressed tumors, recurrence occurred in 5/6 saline and 3/8 MnBuOE mice, with all tumors returning within the same time frame. For 5x9Gy, the regression rates were 7/8 and 8/8 for saline and MnBuOE, respectively, but recurrence occurred in 4/7 saline mice (at days 26, 29, 33 and 37) compared to 1/8 MnBuOE mice (on day 44). Two tumors regressed and recurred in the 5x10Gy saline group, whereas all tumors regressed and did not return in the 5x10Gy MnBuOE group. Mice were followed for 90 days following the start of RT, and their status at day 90 is shown in Supplemental Figure 3b.

To calculate the dose modifying factor (DMF) of this drug, we used logistic regression to estimate the dose of radiation that yields 50% local tumor control for radiation alone and radiation + MnBuOE (Figure 5b). The dose response curves for both study arms were well approximated by logistic curves with comparable steepness (Figure 5b). The TCD_{50} (midpoints) for the saline and MnBuOE arms were 46.5±0.25 and 37.1±0.9 Gy, respectively. The dose modifying factor, defined as the ratio of doses to achieve 50% local tumor control for radiotherapy alone/radiotherapy+MnBuOE, was 1.3.

To investigate the potential mechanisms for the radiosensitizing properties of MnBuOE, we used immunohistochemistry to examine key parameters in tumors treated with 0 or 5x5Gy in the presence of either saline or MnBuOE. First, although RT increased necrosis in both groups (p=0.03), MnBuOE was no different from saline. (Figure 6a). Neither RT nor MnBuOE affected microvessel density (assessed by CD31 expression) (Figure 6b). We next quantified tumor-associated macrophages (TAMs) according to the pan-macrophage marker CD68, with the hypothesis that RT+MnBuOE tumors would show a decrease in TAM numbers. Contrary to our hypothesis, we found that MnBuOE significantly increased $CD68^+$ macrophages in the MnBuOE tumors (p=0.01) (Figure 6c). However, there was a 35% increase in the number of $CD80^+$ M1 macrophages in the MnBuOE tumors in the 5x5Gy group compared with saline + radiation (p=0.03) (Figure 6d). The M1 macrophage phenotype is known to drive a proinflammatory, antitumor immune response[21].

Discussion

The aim of radioprotective drugs is to protect normal tissue, but not tumor. This has been an ongoing concern for the clinical use of amifostine, despite the publication of a meta-analysis which did not show any evidence of tumor radioprotection[22,23]. This study demonstrates that MnBuOE safely and significantly preserves salivary function and reduces mucositis in mice. The dose modifying factor for xerostomia was 0.77. Furthermore, MnBuOE-sensitized FaDu xenografts to RT- the mice that were treated with RT+MnBuOE increased tumor radiosensitivity compared to irradiated mice that did not receive the drug. Analysis of dose response curves indicated a dose modifying factor of 1.3, in favor of RT+MnBuOE compared with RT+saline. This finding aligns with previous studies showing Mn porphyrins radiosensitized mammary and brain tumor models[24,25]. Others have postulated that Mn porphyrins may have divergent effects in normal and tumor tissues due to differences in their baseline redox environments[26]. It is important to note that while we are not the first group to quantify the magnitude of tumor radiosensitization vs. normal tissue radioprotection by Mn porphyrins, we evaluated both endpoints using multiple RT doses +/− MnBuOE. These data was used to determine the extent of normal tumor protection and tumor sensitization.

Evidence for Mn porphyrin protection against RT-induced fibrosis has been mixed. It has been reported that RT-induced increases in penile tissue fibrosis were abrogated by MnTE-2-Pyp, but this study did not include quantification of the images or statistical analysis of the magnitude of radioprotection[9]. Neither MnTE-2-Pyp nor MnTnHex-2-PyP significantly reduced the amount of fibrotic tissue in a lung RT model[14]. Future studies may demonstrate whether protection against fibrosis is a unique element of MnBuOE treatment, or if salivary tissue is merely an easier tissue to protect from fibrosis compared that of penis and lung.

Due to the design of the tumor control study, we did not sample tumors at various times post-RT, and thus our only snapshot of the cell populations within them is when they were collected at $1500mm^3$. Nevertheless, the macrophage populations at endpoint may point to a mechanism by which tumor growth was slowed following MnBuOE+RT. The traditional view of tumor-associated macrophages (TAMs) is negative; their accumulation has been

associated with worse clinical outcome[27]. TAMs enhance tumor growth through production of IL-10, promoting angiogenesis, and secreting proteases that facilitate tumor invasion (reviewed in[28]). However, environmental cues can polarize macrophages towards an M1 (classical) or M2 (alternative) phenotype[21]. For example, M2-skewing can result from increased lactic acid in tumors[29], and Chiang et al. showed that M2 TAMs accumulate in hypoxic tumor regions[30]. Analogues of MnBuOE have been shown to reduce HIF-1 expression[31] and oxidative stress[32]. Taken together, these findings support a hypothesis that a MnBuOE-mediated reduction in tumor hypoxia prevents TAMs from acquiring the M2 phenotype. The retention of the tumoricidal M1 phenotype in our study was associated with delayed tumor growth following RT. Future studies could address this hypothesis by monitoring tumor oxidative stress following RT, or by assessing the functional phenotype of macrophages through analysis of intratumoral cytokines and NK cell numbers.

The major human salivary glands consist of the parotid, submandibular and sublingual glands, located throughout the upper neck region[33]. Often, these glands receive high doses of irradiation because of their close proximity to target volumes in patients with head and neck cancer. Mean doses >26Gy usually lead to permanent loss of saliva production[34]. Techniques such as intensity modulated radiation therapy (IMRT) can minimize the amount of radiation delivered to the glands, with varying degrees of success. However, IMRT has its own risks, including marginal miss, which may lead to tumor recurrence[35,36]. Furthermore, even with the use of IMRT, a significant proportion of patients still develop long term xerostomia[37]. Even “dose sparing” approaches that preferentially minimize radiation to one of the two parotid glands may reduce salivary output of the *spared* gland by up to 50%[38]. Clearly, alternative therapies are needed.

The only FDA-approved radioprotective drug for xerostomia is amifostine, a free radical scavenger. Unfortunately, the side effects of amifostine include hypotension, nausea and vomiting[3], and it is not approved for use in preventing mucositis. Furthermore, amifostine does not completely protect all patients. The incidence of grade ≥2 xerostomia at one year post-treatment was 51% in amifostine-treated patients compared to 78% in control patients[4]. A follow-up study reported that at 18 months post-treatment, the incidence of grade ≥2 xerostomia in patients receiving amifostine was still 29% (compared to 52% of control patients) and only 68% of amifostine-treated patients could produce >0.1 g saliva in 5 minutes without stimulation (compared to 59% of control patients)[5].

Amifostine is a stoichiometric scavenger of ROS, while MnBuOE catalytically inactivates a wide range of ROS. Moreover, given its lipophilic nature and pentacationic charge, it accumulates in mitochondria, an important site of radiation damage[8]. RT results in chronic oxidative stress due to mitochondrial damage in normal tissue[8]. We have previously shown that a single dose of Mn porphyrins given at the moment of injury suppresses the damage for only a limited period of time[13]. In contrast, when given for at least a week or longer Mn porphyrins reduced RT-driven oxidative stress[13] and protected lung against RT-induced injury. In our study, MnBuOE protected mice from RT-induced xerostomia with a dose-modifying factor of 0.77.

Conclusion

This study demonstrates that MnBuOE provides radioprotection against salivary gland and mucosal injury in a rodent model. Further, MnBuOE was clearly shown to be a tumor radiosensitizer. These encouraging preclinical data suggest that clinical development of MnBuOE is worthwhile.

Supplementary Material

Refer to Web version on PubMed Central for supplementary material.

Acknowledgements

We thank Irene Li and Giao Nguyen for assistance with irradiation and dosimetry, and Alina Boico and Chen-Ting Lee for assistance with immmunofluorescence microscopy.

Funding

This work was supported by Wallace H. Coulter Foundation (IS, IBH, MWD); the National Institute of Health (grant CA40355 [MWD]); the North Carolina Biotechnology Center; and BioMimetix LLC (KAA, AT, IS, IBH, MWD). MKB was supported by T32OD011130.

IBH and IS are consultants with BioMimetix JVLLC (USA) and hold equities in BioMimetix JVLLC. IBH and IS and Duke University have patent rights and have licensed technologies to BioMimetix JVLLC.

References

1. Al-Mamgani A, Mehilal R, van Rooij PH, Tans L, Sewnaik A, Levendag PC. Toxicity, quality of life, and functional outcomes of 176 hypopharyngeal cancer patients treated by (chemo)radiation: the impact of treatment modality and radiation technique. The Laryngoscope. 2012; 122(8):1789–1795. [PubMed: 22833307]
2. Sonis ST, Oster G, Fuchs H, et al. Oral mucositis and the clinical and economic outcomes of hematopoietic stem-cell transplantation. Journal of clinical oncology : official journal of the American Society of Clinical Oncology. 2001; 19(8):2201–2205. [PubMed: 11304772]
3. Rades D, Fehlauer F, Bajrovic A, Mahlmann B, Richter E, Alberti W. Serious adverse effects of amifostine during radiotherapy in head and neck cancer patients. Radiother Oncol. 2004; 70(3):261–264. [PubMed: 15064010]
4. Brizel DM, Wasserman TH, Henke M, et al. Phase III randomized trial of amifostine as a radioprotector in head and neck cancer. Journal of clinical oncology : official journal of the American Society of Clinical Oncology. 2000; 18(19):3339–3345. [PubMed: 11013273]
5. Wasserman TH, Brizel DM, Henke M, et al. Influence of intravenous amifostine on xerostomia, tumor control, and survival after radiotherapy for head-and- neck cancer: 2-year follow-up of a prospective, randomized, phase III trial. Int J Radiat Oncol Biol Phys. 2005; 63(4):985–990. [PubMed: 16253773]
6. Hanaue N, Takeda I, Kizu Y, Tonogi M, Yamane GY. Peroxynitrite formation in radiation-induced salivary gland dysfunction in mice. Biomed Res. 2007; 28(3):147–151. [PubMed: 17625347]
7. Rajic Z, Tovmasyan A, Spasojevic I, et al. A new SOD mimic, Mn(III) ortho N-butoxyethylpyridylporphyrin, combines superb potency and lipophilicity with low toxicity. Free Radic Biol Med. 2012; 52(9):1828–1834. [PubMed: 22336516]
8. Kim GJ, Fiskum GM, Morgan WF. A role for mitochondrial dysfunction in perpetuating radiation-induced genomic instability. Cancer research. 2006; 66(21):10377–10383. [PubMed: 17079457]
9. Oberley-Deegan RE, Steffan JJ, Rove KO, et al. The antioxidant, MnTE-2-PyP, prevents side-effects incurred by prostate cancer irradiation. PloS one. 2012; 7(9):e44178. [PubMed: 22984473]

10. Dogan S, Unal M, Ozturk N, et al. Manganese porphyrin reduces retinal injury induced by ocular hypertension in rats. Experimental eye research. 2011; 93(4):387–396. [PubMed: 21669199]
11. Dorai T, Fishman AI, Ding C, Batinic-Haberle I, Goldfarb DS, Grasso M. Amelioration of renal ischemia-reperfusion injury with a novel protective cocktail. The Journal of urology. 2011; 186(6): 2448–2454. [PubMed: 22019164]
12. Yakovlev VA, Rabender CS, Sankala H, et al. Proteomic analysis of radiation-induced changes in rat lung: Modulation by the superoxide dismutase mimetic MnTE-2-PyP(5+). Int J Radiat Oncol Biol Phys. 2010; 78(2):547–554. [PubMed: 20584581]
13. Gauter-Fleckenstein B, Fleckenstein K, Owzar K, et al. Early and late administration of MnTE-2-PyP5+ in mitigation and treatment of radiation-induced lung damage. Free Radic Biol Med. 2010; 48(8):1034–1043. [PubMed: 20096348]
14. Gauter-Fleckenstein B, Fleckenstein K, Owzar K, Jiang C, Batinic-Haberle I, Vujaskovic Z. Comparison of two Mn porphyrin-based mimics of superoxide dismutase in pulmonary radioprotection. Free Radic Biol Med. 2008; 44(6):982–989. [PubMed: 18082148]
15. Sheng H, Spasojevic I, Warner DS, Batinic-Haberle I. Mouse spinal cord compression injury is ameliorated by intrathecal cationic manganese(III) porphyrin catalytic antioxidant therapy. Neuroscience letters. 2004; 366(2):220–225. [PubMed: 15276251]
16. Clarkson R, Lindsay PE, Ansell S, et al. Characterization of image quality and image-guidance performance of a preclinical microirradiator. Medical physics. 2011; 38(2):845–856. [PubMed: 21452722]
17. Jonjic, S. Surgical removal of mouse salivary glands. In: Coligan, John E., et al., editors. Current protocols in immunology. Vol. Chapter 1. 2001. p. 11
18. Alamir I, Boukhettala N, Aziz M, Breuille D, Dechelotte P, Coeffier M. Beneficial effects of cathepsin inhibition to prevent chemotherapy-induced intestinal mucositis. Clinical and experimental immunology. 2010; 162(2):298–305. [PubMed: 20731673]
19. Klein, J.; Moeschberger, K. Survival Analysis: Techniques for Censored and Truncated Data. 2ed. Springer; 2005.
20. Bentzen SM, Tucker SL. Quantifying the position and steepness of radiation dose-response curves. International Journal of Radiation Biology. 1997; 71(5):531–542. [PubMed: 9191898]
21. Sica A, Mantovani A. Macrophage plasticity and polarization: in vivo veritas. The Journal of clinical investigation. 2012; 122(3):787–795. [PubMed: 22378047]
22. Lindegaard JC, Grau C. Has the outlook improved for amifostine as a clinical radioprotector? Radiother Oncol. 2000; 57(2):113–118. [PubMed: 11054513]
23. Bourhis J, Blanchard P, Maillard E, et al. Effect of amifostine on survival among patients treated with radiotherapy: a meta-analysis of individual patient data. Journal of clinical oncology : official journal of the American Society of Clinical Oncology. 2011; 29(18):2590–2597. [PubMed: 21576630]
24. Moeller BJ, Batinic-Haberle I, Spasojevic I, et al. A manganese porphyrin superoxide dismutase mimetic enhances tumor radioresponsiveness. Int J Radiat Oncol Biol Phys. 2005; 63(2):545–552. [PubMed: 16168847]
25. Weitzel DH, Tovmasyan A, Ashcraft KA, et al. Radioprotection of the brain white matter by Mn(III) n-Butoxyethylpyridylporphyrin-based superoxide dismutase mimic MnTnBuOE-2-PyP5+ Molecular cancer therapeutics. 2015; 14(1):70–79. [PubMed: 25319393]
26. Batinic-Haberle I, Spasojevic I. Complex chemistry and biology of redox-active compounds, commonly known as SOD mimics, affect their therapeutic effects. Antioxidants & redox signaling. 2014; 20(15):2323–2325. [PubMed: 24650329]
27. Mahmoud SM, Lee AH, Paish EC, Macmillan RD, Ellis IO, Green AR. Tumour-infiltrating macrophages and clinical outcome in breast cancer. Journal of clinical pathology. 2012; 65(2): 159–163. [PubMed: 22049225]
28. Pollard JW. Tumour-educated macrophages promote tumour progression and metastasis. Nature reviews. Cancer. 2004; 4(1):71–78. [PubMed: 14708027]
29. Colegio OR, Chu NQ, Szabo AL, et al. Functional polarization of tumour-associated macrophages by tumour-derived lactic acid. Nature. 2014

30. Chiang CS, Fu SY, Wang SC, et al. Irradiation promotes an m2 macrophage phenotype in tumor hypoxia. Frontiers in oncology. 2012; 2:89. [PubMed: 22888475]
31. Gridley DS, Makinde AY, Luo X, et al. Radiation and a metalloporphyrin radioprotectant in a mouse prostate tumor model. Anticancer research. 2007; 27(5A):3101–3109. [PubMed: 17970050]
32. Moeller BJ, Cao Y, Li CY, Dewhirst MW. Radiation activates HIF-1 to regulate vascular radiosensitivity in tumors: role of reoxygenation, free radicals, and stress granules. Cancer cell. 2004; 5(5):429–441. [PubMed: 15144951]
33. van de Water TA, Bijl HP, Westerlaan HE, Langendijk JA. Delineation guidelines for organs at risk involved in radiation-induced salivary dysfunction and xerostomia. Radiother Oncol. 2009; 93(3):545–552. [PubMed: 19853316]
34. Eisbruch A, Ten Haken RK, Kim HM, Marsh LH, Ship JA. Dose, volume, and function relationships in parotid salivary glands following conformal and intensity-modulated irradiation of head and neck cancer. Int. J. Radiation Oncology Biol. Phys. 1999; 45(3):577–587.
35. Dawson LA, Anzai Y, Marsh L, et al. Patterns of local-regional recurrence following parotid-sparing conformal and segmental intensity-modulated radiotherapy for head and neck cancer. Int J Radiat Oncol Biol Phys. 2000; 46(5):1117–1126. [PubMed: 10725621]
36. Cannon DM, Lee NY. Recurrence in region of spared parotid gland after definitive intensity-modulated radiotherapy for head and neck cancer. Int J Radiat Oncol Biol Phys. 2008; 70(3):660–665. [PubMed: 18037580]
37. Wang R, Wu F, Lu H, et al. Definitive intensity-modulated radiation therapy for nasopharyngeal carcinoma: long-term outcome of a multicenter prospective study. Journal of cancer research and clinical oncology. 2012
38. Eisbruch A, Ship JA, Martel MK, et al. Parotid gland sparing in patients undergoing bilateral heand and neck irradiation: techniques and early results. Int. J.Radiation Oncology Biol. Phys. 1996; 36(2):469–480.

Summary

We demonstrate that a novel Mn-porphyrin oxidative stress modifier, Mn(III) *meso*-tetrakis(*N*-n-butoxyethylpyridinium-2-yl)porphyrin (MnBuOE,) widens the therapeutic margin in a pre-clinical head and neck cancer model. MnBuOE sensitizes tumors to fractionated radiation, with a dose modifying factor of 1.3, while significantly reducing mucositis, xerostomia and salivary gland fibrosis.

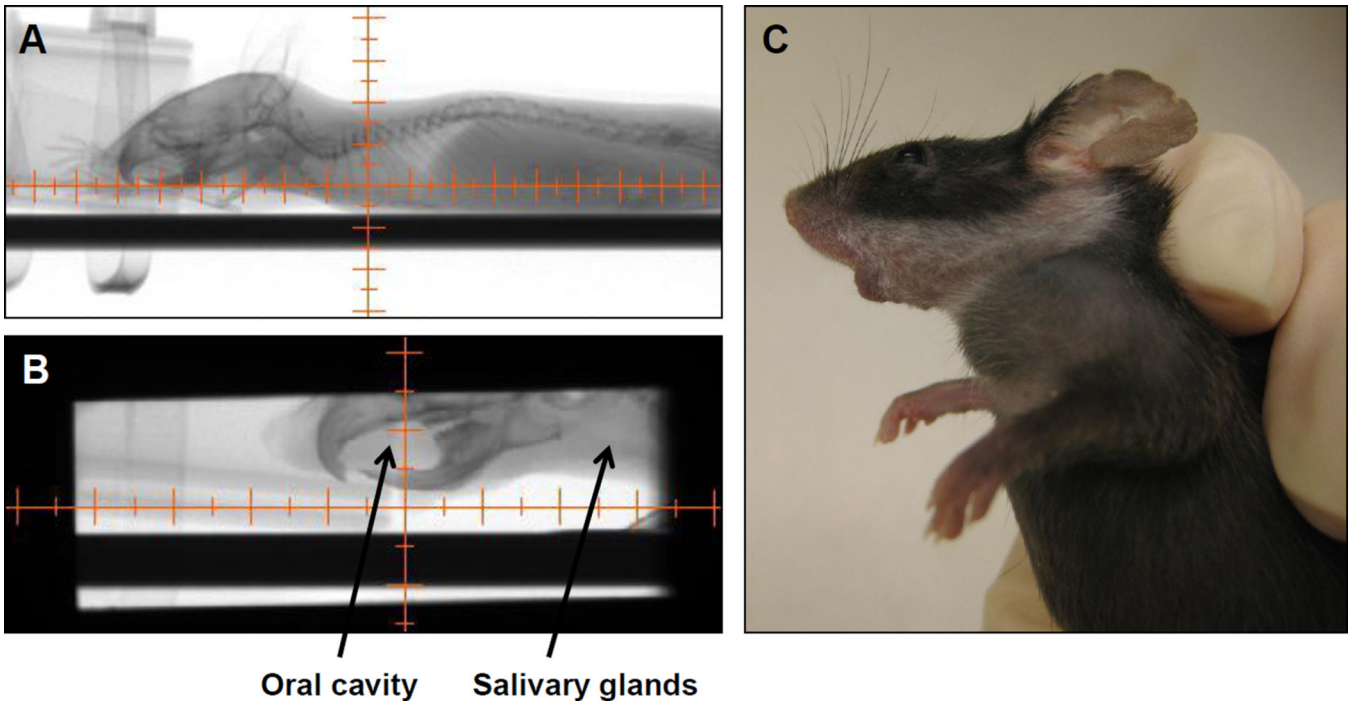

Figure 1.

Irradiation using the X-RAD 225Cx small animal irradiator. A: Mice were visualized using the fluoroscopy settings. B: The collimator's isocenter was placed in a position that targeted radiation beam to include the oral cavity and salivary glands while excluding the eyes and central nervous system. C: The resulting leukotrichia post-RT, reflecting the precision of the radiation beam.

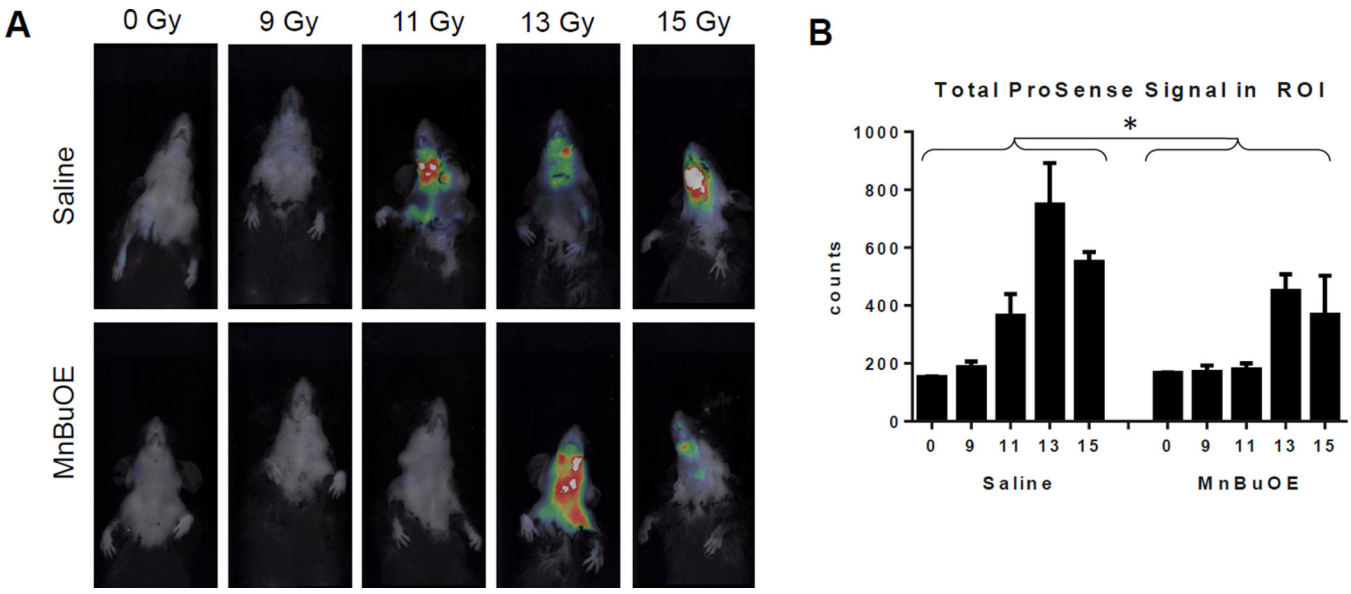

Figure 2.

Incidence and severity of mucositis ten days post-RT. A: Representative mouse from each of the treatment groups. B: For signal quantification, the same size region of interest was drawn around the irradiation field of each mouse. The amount of activated ProSense 750EX was quantified in terms of energy using TrueQuant software. N=3/group. Error bars represent the standard error. *p=0.009

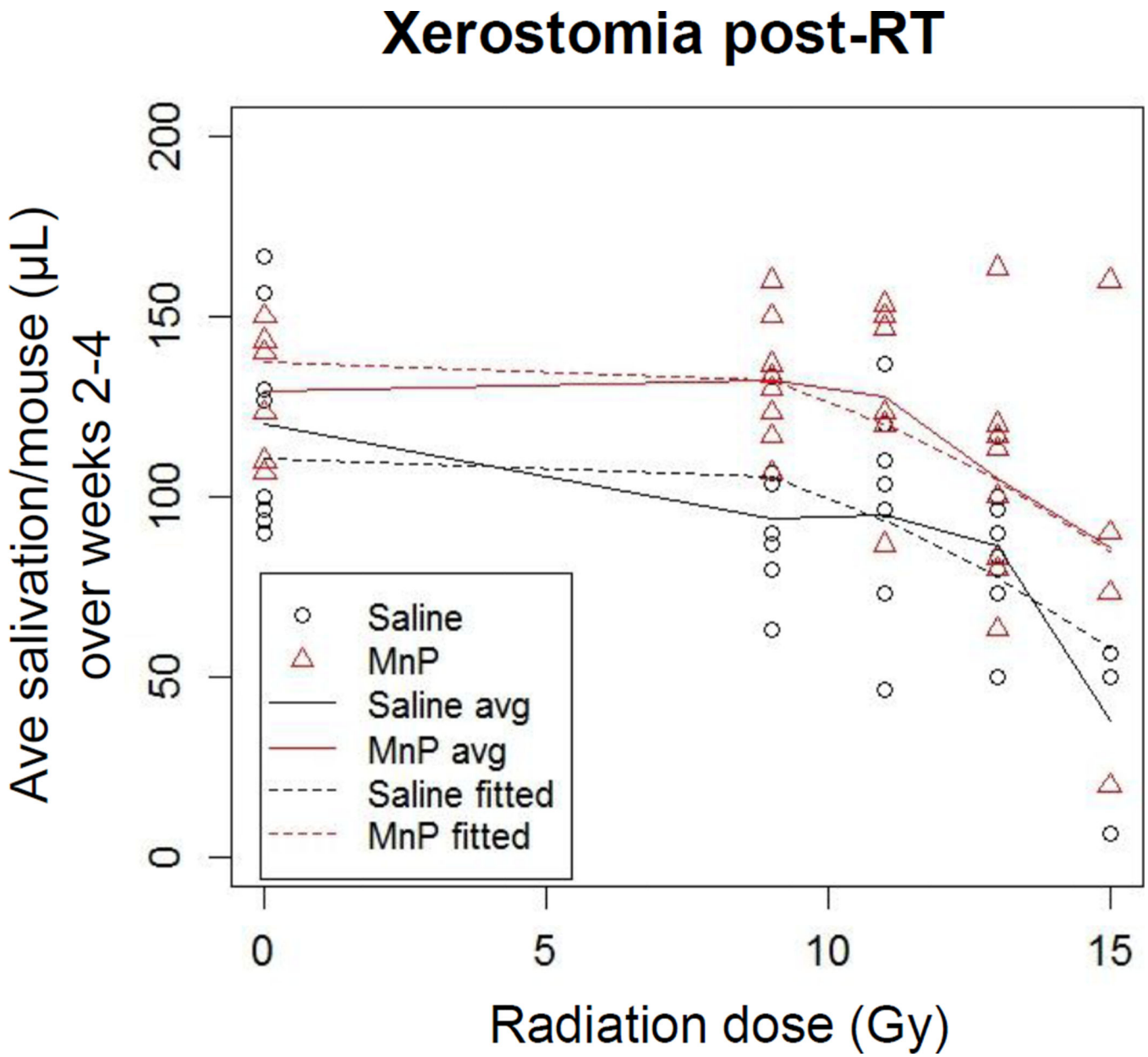

Figure 3.

Reduction of saliva production. Stimulated saliva was collected weekly following RT. Saliva production by each mouse was averaged for weeks 2–4 post-RT. For the 15Gy groups, only 3 mice/group survived the acute effects of radiation; N=8 for all other groups. p=0.0002

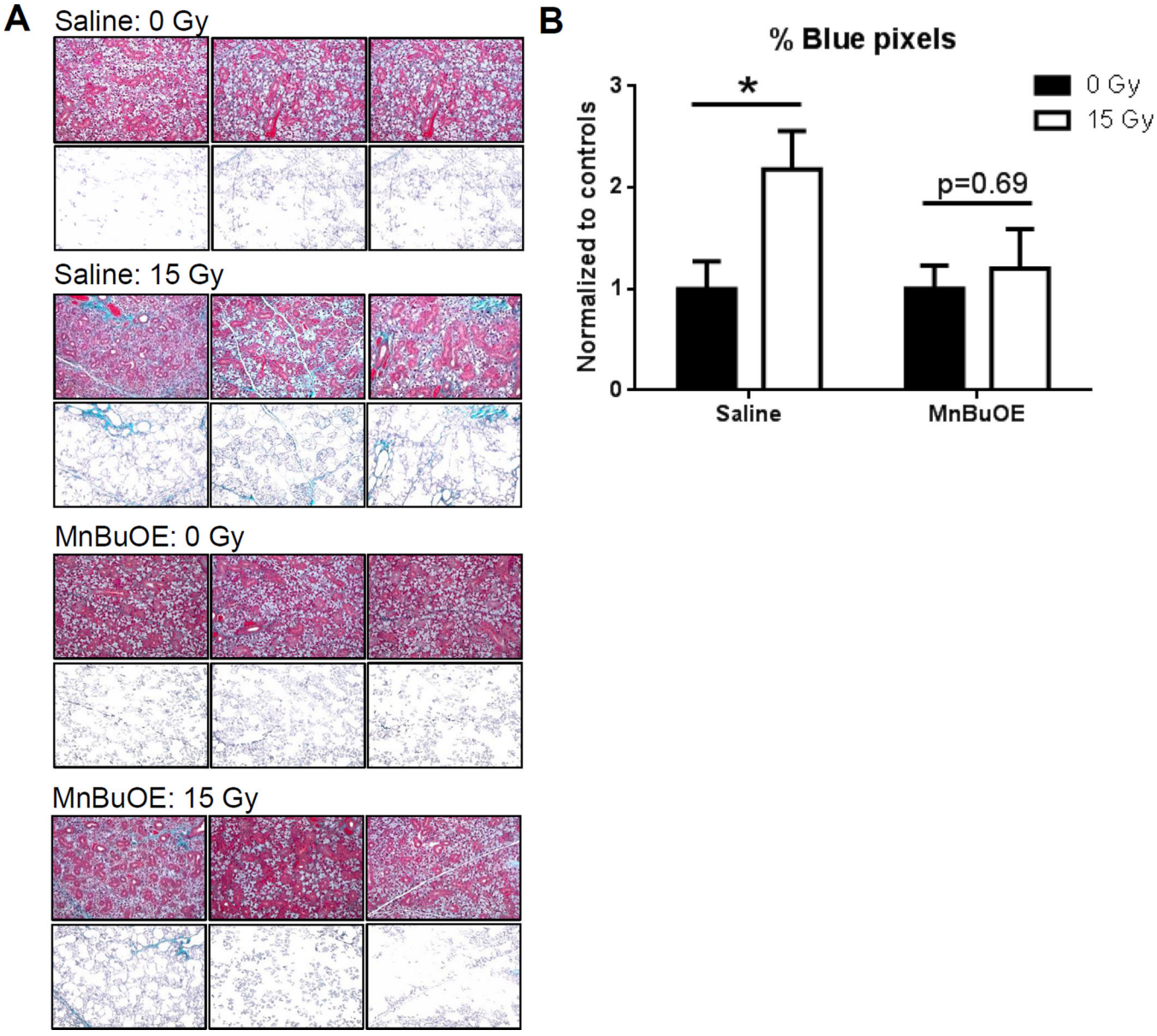

Figure 4.

Fibrotic tissue in the salivary gland six weeks post-RT. A: Images of Masson's trichrome-stained submandibular glands (top panels) were processed using MATLAB to show only the blue pixels that also had a green:red ratio >0.1 (bottom panels). Representative images from three mice per treatment group are shown. B: Quantified Masson's staining expressed as the ratio of blue:red pixels in each image. N=3–7/group. Error bars represent the standard error. *p=0.009

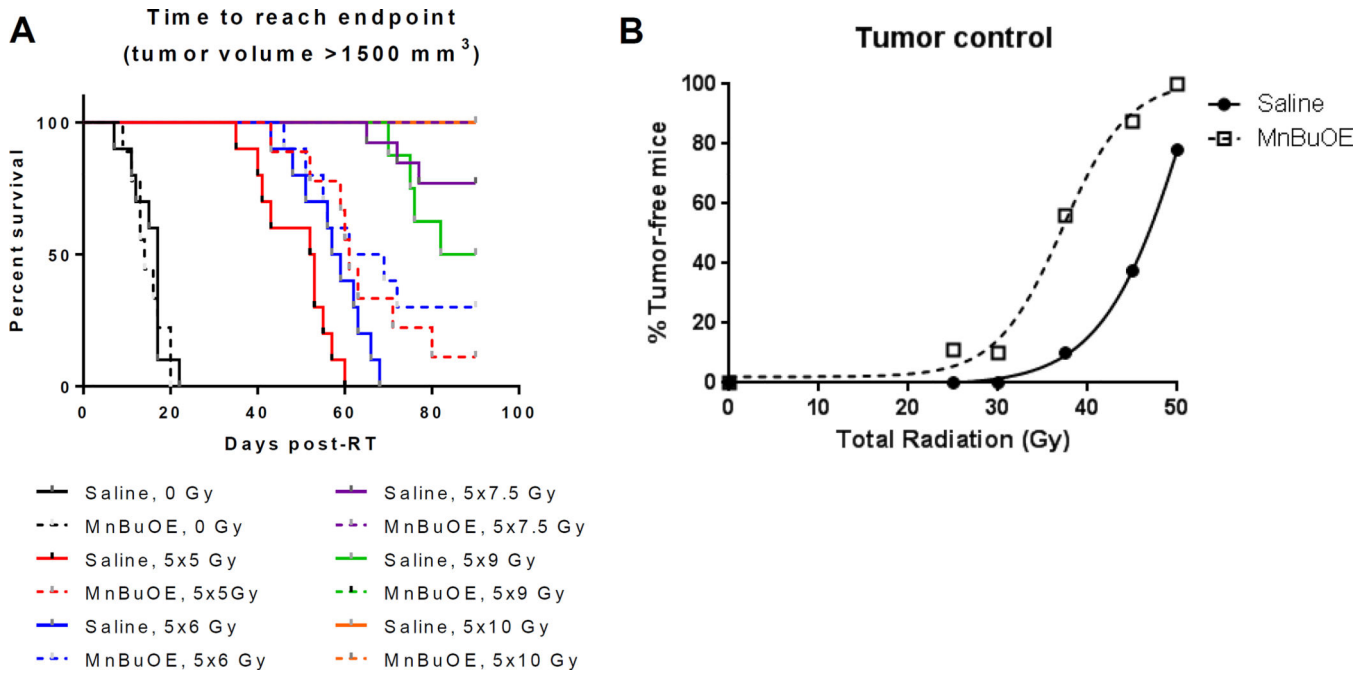

Figure 5.

Tumor control study using FaDu xenografts and fractionated radiation. A: Survival curves for FaDu tumor-bearing mice to reach humane endpoint following RT, with either saline or MnBuOE administered concomitantly. B: Radiation dose response curves showing the percentage of mice that were cured, i.e., tumors regressed completely and did not return by 90 days post-RT. N=6–10/groups. p=0.02

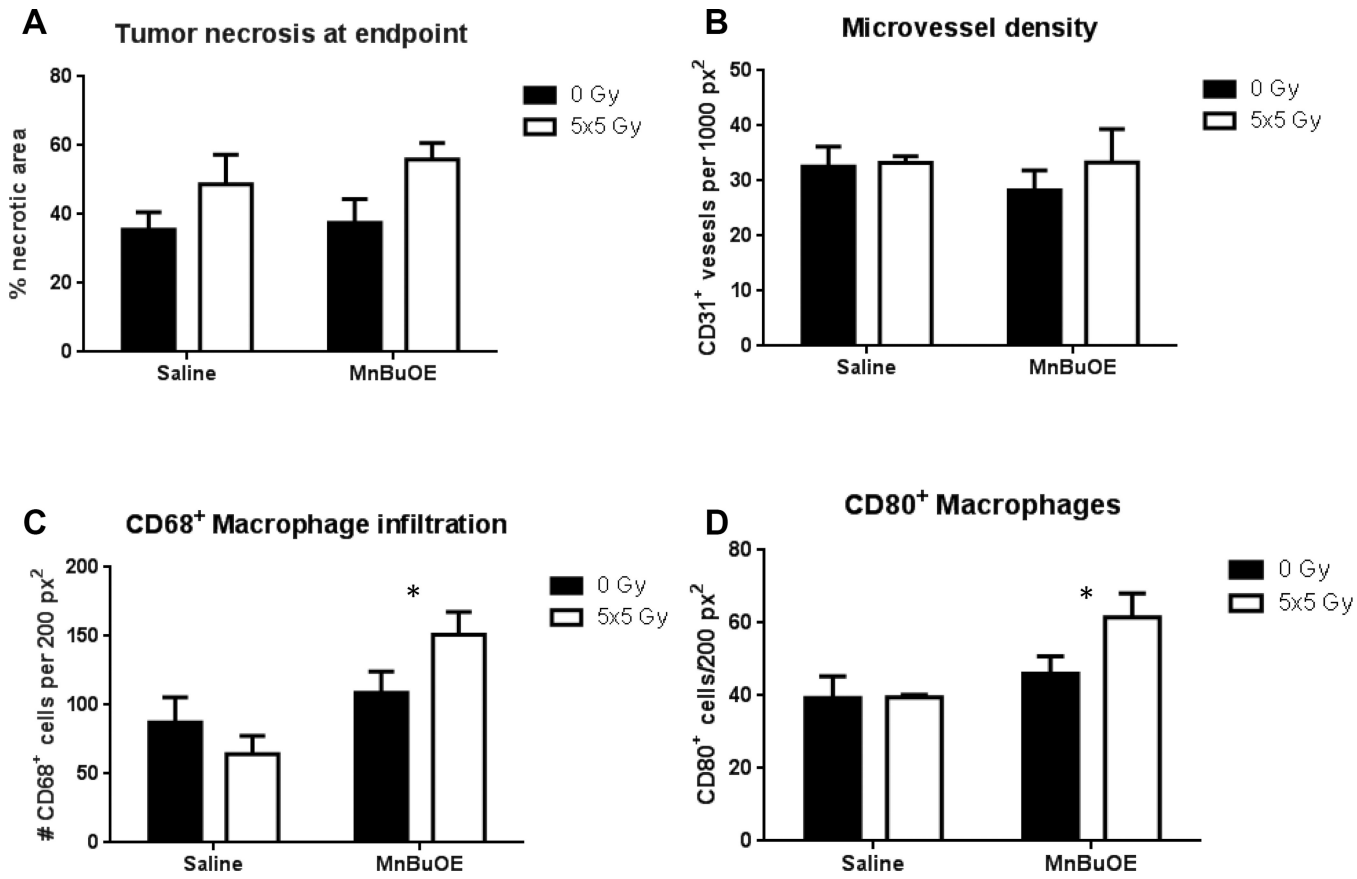

Figure 6.

Immunohistochemistry of tumors taken at endpoint (volume >1500 mm^3). A: Percentage of tumor that was necrotic. B: Microvessel density. C: Macrophage infiltration, using CD68 as a pan-macrophage surface marker. p=0.01 D: M1 macrophage infiltration, using CD80 as the identifying surface marker p=0.03. N=3–6/group. Error bars represent the standard error.